Highly Uniform TiO_2/SnO_2/Carbon Hybrid Nanofibers with Greatly Enhanced Lithium Storage Performance

Zunxian Yang,[*1] Qing Meng,[2] Zaiping Guo,[*2,3] Xuebin Yu,[*4] Tailiang Guo,[1] Rong Zeng[5]

[1] National & Local United Engineering Laboratory of Flat Panel Display Technology, Fuzhou University, Fuzhou 350002, P. R. China

[2]Institute for Superconducting & Electronic Materials, University of Wollongong, NSW 2522, Australia

[3]School of Mechanical, Materials & Mechatronics Engineering, University of Wollongong, NSW 2522, Australia

[4]Department of Materials Science, Fudan University, Shanghai 200433, P. R. China

[5]School of Computing, Engineering and Mathematics, University of Western Sydney, NSW 2751, Australia,

Supporting Information

Captions

Fig. S1 TGA results for **(a) TSC1**, **(b) TSC2**, **(c) TSC3.**

Fig. S2 Low and high (insets) magnification FE-SEM images of the hybrid nanofibers: **(a) TSC1**; **(b) TS1**; **(c) TSC2**; **(d) TS2**; **(e) TSC3**; **(f) TS3**. (The hybrid nanofibers of

* Corresponding author should be addressed. Tel.: +61 2 4221 5225; Fax: +61 2 4221 5731

E-mail: zguo@uow.edu.au (Z. Guo)

yangzunxian@hotmail.com (Z. Yang)

yuxuebin@fudan.edu.cn (X. Yu)

TSC1, **TSC2,** and **TSC3** are smoother and slightly thicker than those of **TS1**, **TS2,** and **TS3** because the carbon matrix has been removed from the **TS1**, **TS2,** and **TS3** nanofibers.)

Fig. S3 (a) Low-magnification TEM image of **TS1**, indicating that there are some short broken nanofibers, possibly owing to the ultrasonic dispersion process during the sample preparation for TEM observations. **(b)** High-magnification TEM image of **TS1**, indicating that there are many rutile TiO_2 nanocrystals in the hybrid nanofibers.

Fig. S4 Energy dispersive X-ray (EDX) spectra and corresponding content tables for the samples (**insets**): **(a) TSC1; (b)TS1; (c)TSC2; (d) TS2; (e)TSC3; (f) TS3.** (Carbon signals in the samples lacking it result from the tape used for SEM observations.)

Fig. S5 XPS high-resolution spectra with curve fitting of **(a)** Ti2p region of **TSC3**, **(b)** Ti2p region of **TS3**, **(c)** Sn3d region of **TSC3**, **(d)** Sn3d region of **TS3**, **(e)** O1s region of **TSC3**, **(f)** O1s region of **TS3**, **(g)** C1s region of **TSC3**.

Fig. S6 Cyclic voltammograms of **TS2** electrode from the first cycle to the fifth cycle at a scan rate of 0.1 mVs^{-1} in the voltage range of 0.01–3.0 V.

Fig. S7 Comparison of cycling performance **(a)** and coulombic efficiency **(b)** of **TSC3** nanofiber electrodes with that of SnO_2/C nanofiber electrodes fabricated using the same technique.

Fig. S8 Nyquist plots of **TS1** and **TSC1** electrodes. The inset shows equivalent circuits for the **TS1** and **TSC1** electrode/electrolyte interfaces.

Table S1 Kinetic parameters of **TS1** and **TSC1** electrodes.

Fig.S9 Charge diffusion and conduction mechanisms of composite nanowires during charge/discharge processes, with the insets showing typical nanofibers:

(a) TSC1, **TSC2**, and **TSC3**; **(b) TS1, TS2**, and **TS3**.

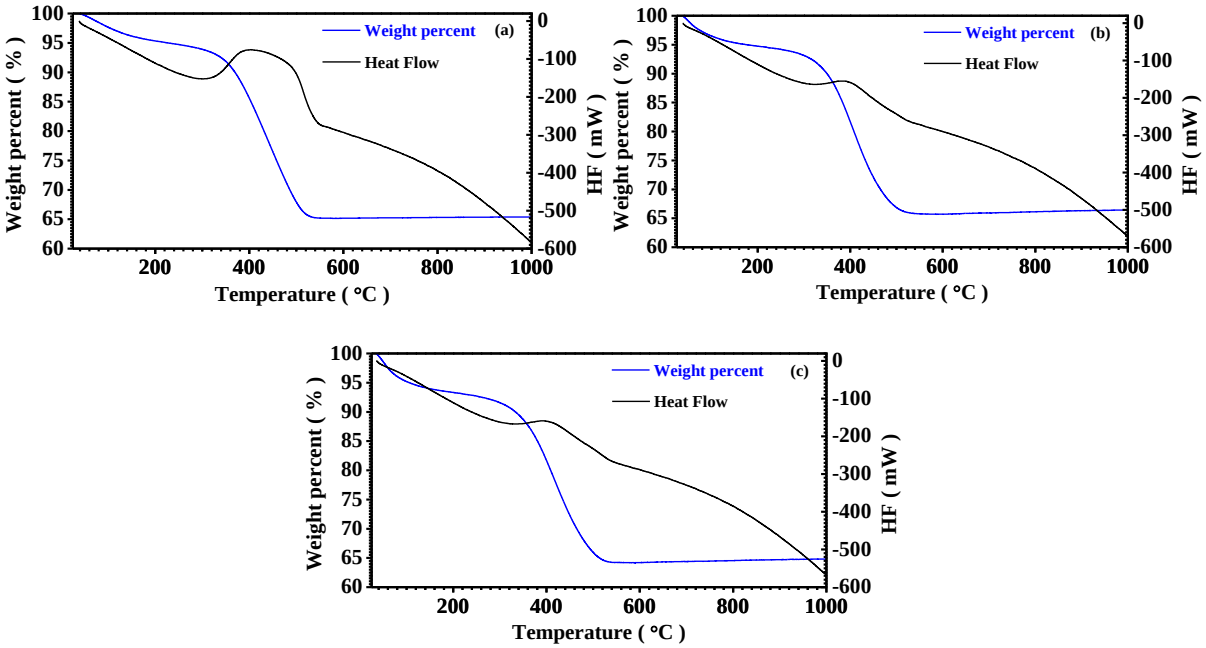

Fig. S1

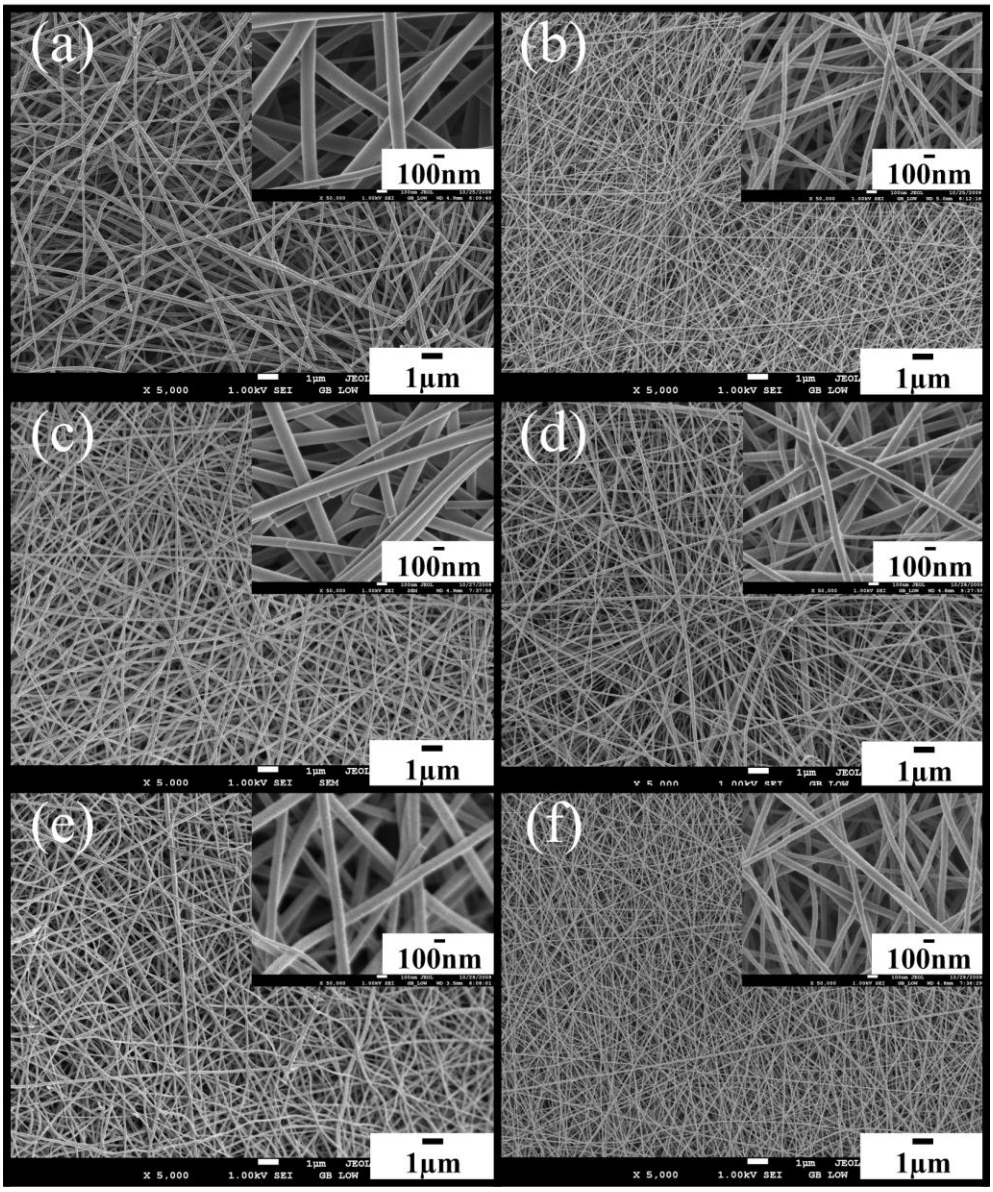

Fig. S2

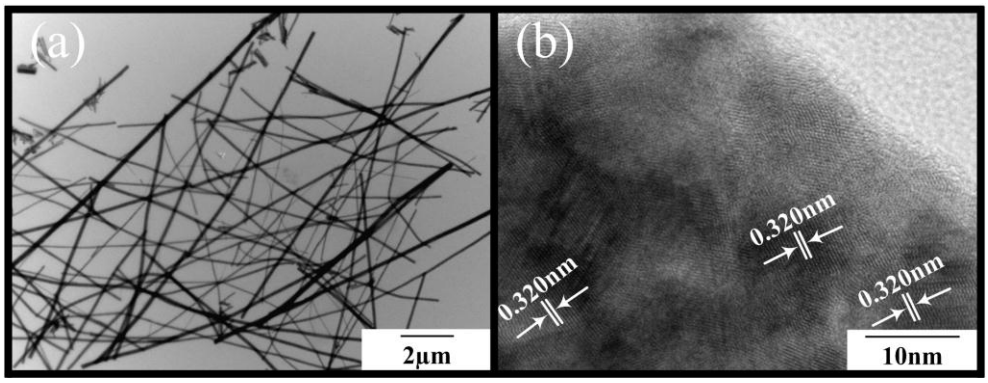

Fig. S3

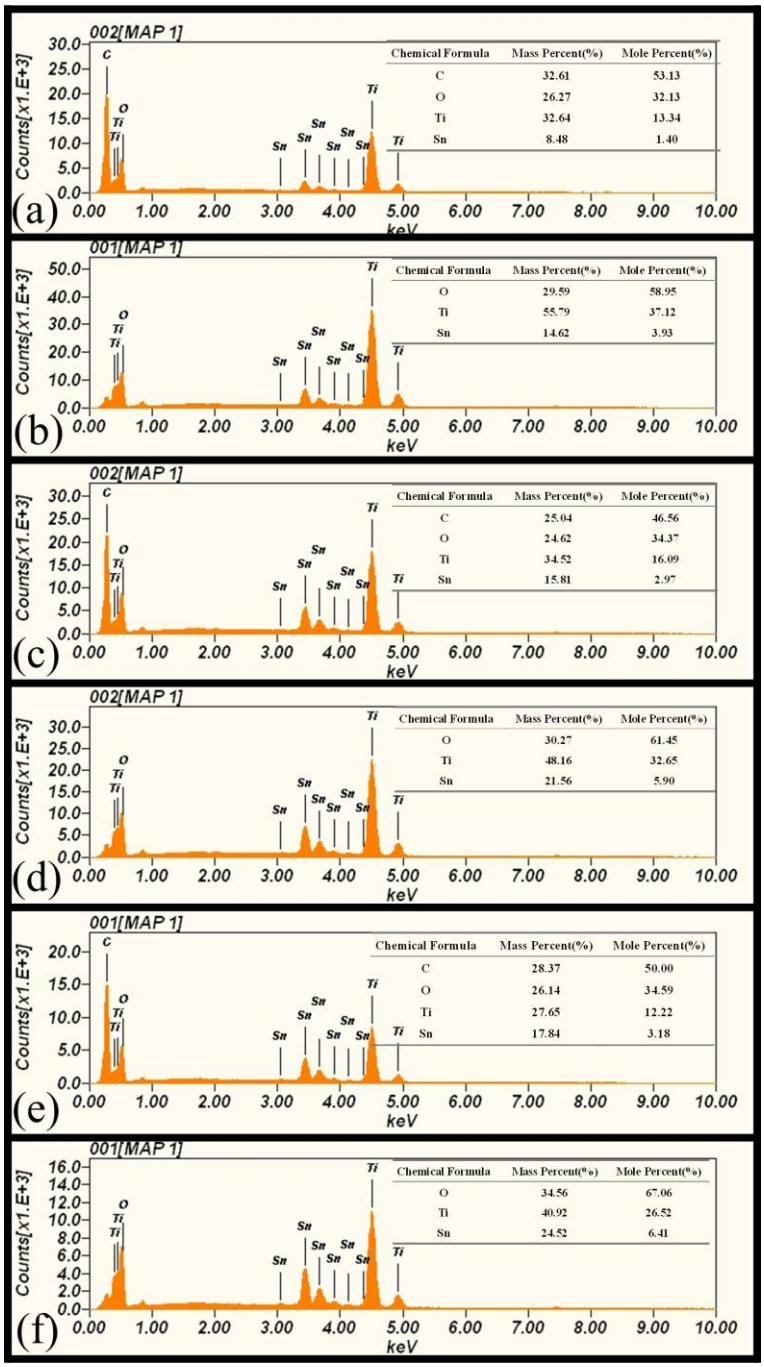

Fig. S4

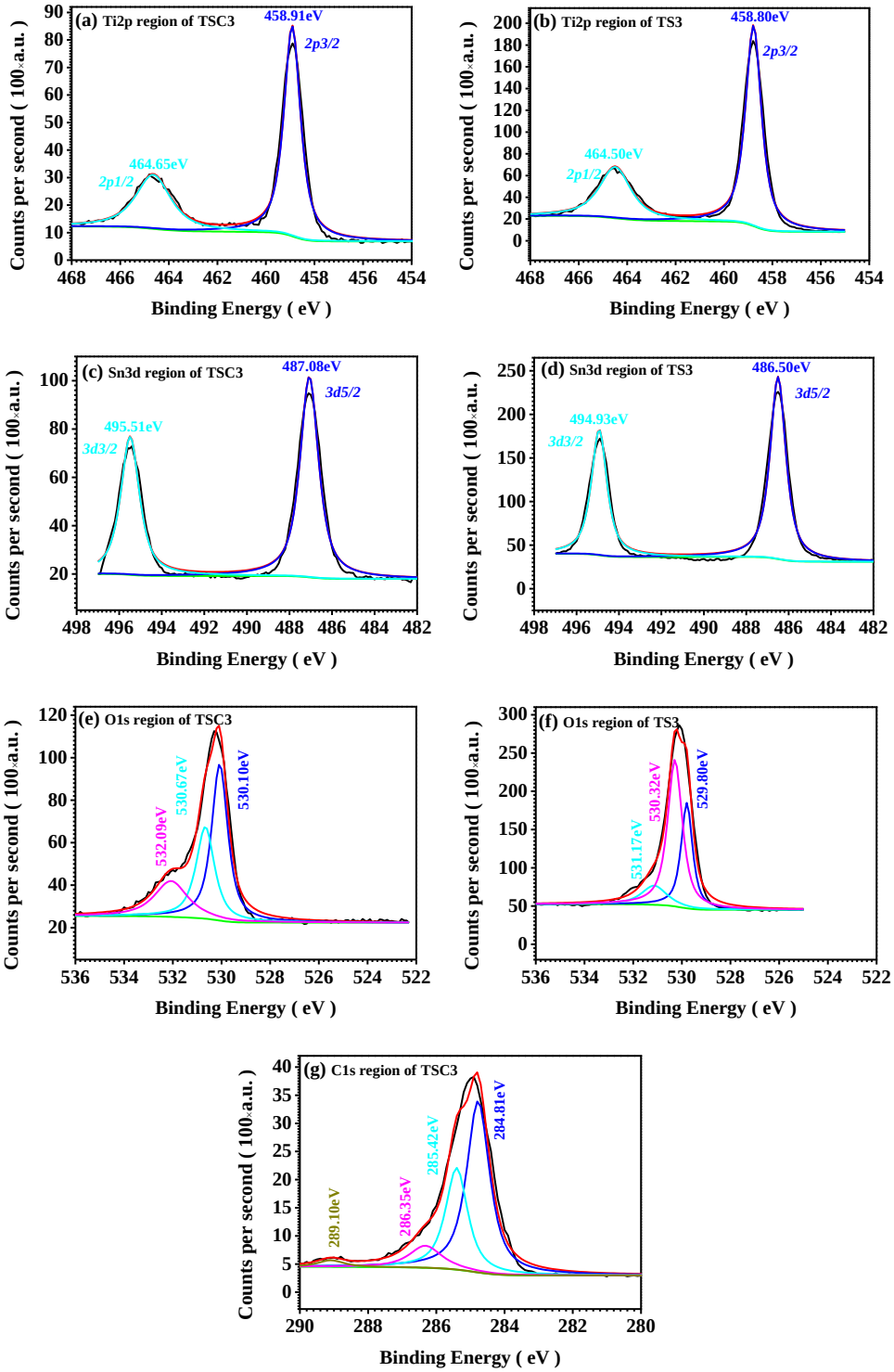

Fig. S5

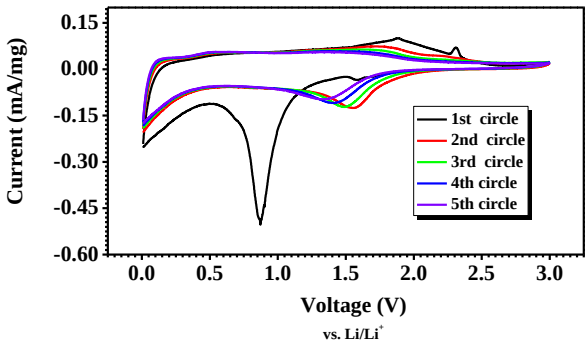

Fig. S6

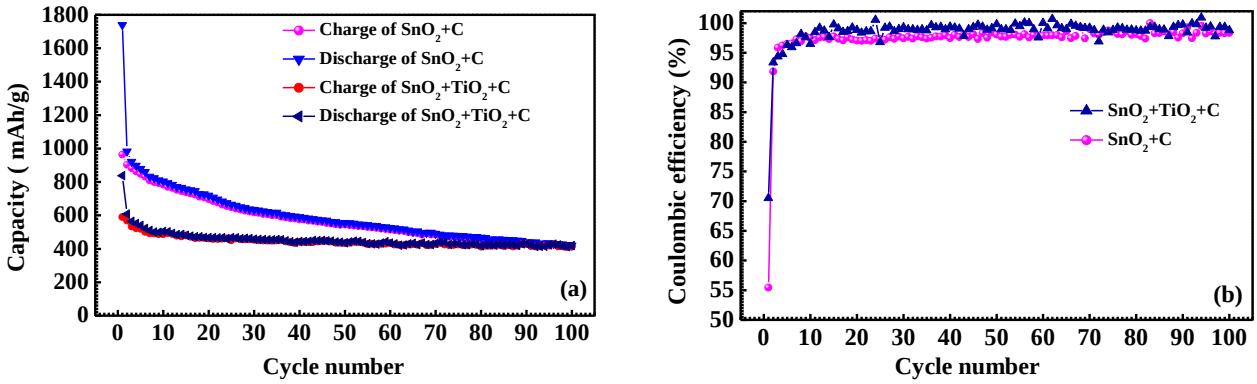

Fig. S7

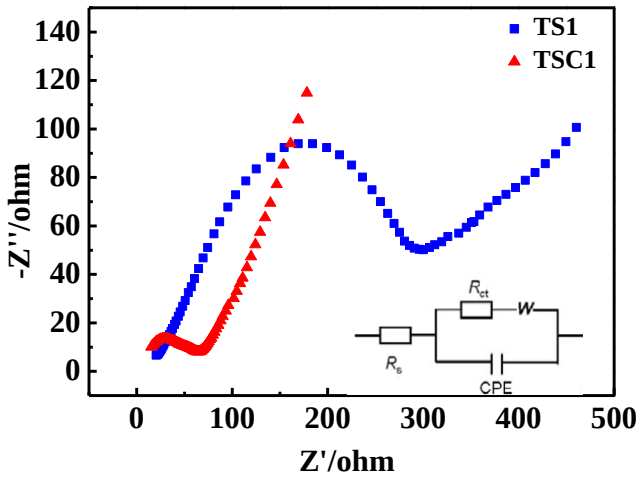

Fig. S8

Table S1

Electrode	R_s (Ω)	CPE (μF)	R_{ct} (Ω)
SnO_2+TiO_2	44.53	7.505	243.1
SnO_2+TiO_2@C	24.29	0.884	38.39

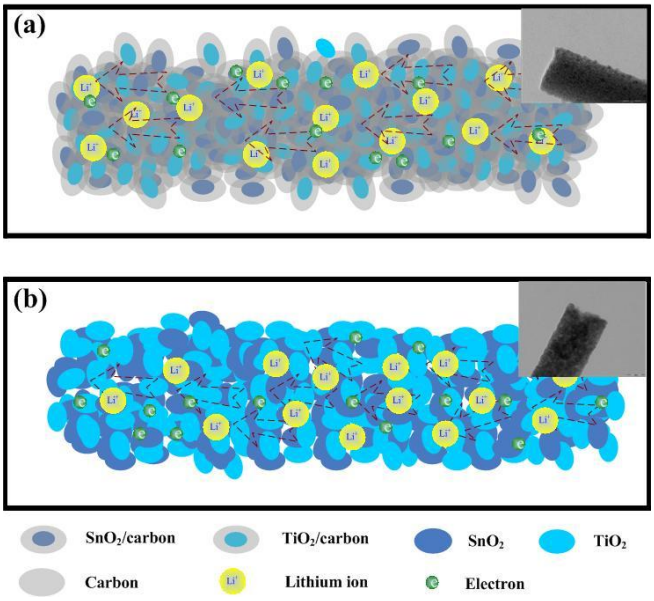

Fig.S9